Spontaneous Lamellar Alignment in Thickness-Modulated Block Copolymer Films

By *Bong Hoon Kim, Hyung Min Lee, Joo-Hyung Lee, Seung-Woo Son, Seong-Jun Jeong, Sumi Lee, Dong Il Lee, Sin Ung Kwak, Hawoong Jeong, Hyunjung Shin, Jun-Bo Yoon, Oleg D. Lavrentovich,* and *Sang Ouk Kim**

Here, spontaneous lamellar alignment in a thickness-modulated block copolymer film is presented as a facile, scalable, and general approach for creating a highly aligned lamellar morphology. Thickness-modulated block copolymer films are prepared on neutral surfaces by various methods, such as solution dropping, dewetting-induced self-organized patterning, and thermal imprinting. Regardless of the film preparation method, the self-assembled lamellar domains become spontaneously aligned along the thickness gradient after sufficient thermal annealing. Real-time AFM imaging reveals that spontaneous alignment occurs through the directional growth of well-ordered domains along the thickness gradient, which is accompanied by defect dynamics, with vertical linear defects moving from thicker parts of the film towards the thinner ones, reducing their length and thus the associated energy. The mechanism underlying this interesting self-aligning behavior is provided by a 'geometric anchoring' phenomenon, originally envisioned to account for the liquid crystal alignment under a non-flat geometry of confinement. This novel self-aligning principle offers a valuable opportunity to control nanoscale alignment in block copolymer films by manipulating the, much larger, microscale morphology.

1. Introduction

Self-assembling materials may provide a highly efficient route to nanofabrication.[1–5] Among various self-assembling materials, block copolymer thin films are of particular technological interest for low-cost, large-area nanopatterning.[6,7] Taking advantage of spontaneous and parallel assembly into nanodomains comprising functional and morphological diversity, a variety of block copolymer lithographic methods have been developed to produce nanopatterned substrates,[8–10] quantum dot arrays,[11–14] metal nanowire arrays,[15,16] and so on. Nevertheless, further progress towards highly advanced applications has been hindered, largely by the poor long-range ordering of nanodomains in spontaneously assembled thin films.

Microphase separation, whereby periodic ordering of block copolymer nanodomains can be generated, is generally mediated by weak forces. As a consequence, long-range

[*] Prof. S. O. Kim, B. H. Kim, H. M. Lee, S.-J. Jeong
Department of Materials Science and Engineering
KI for the Nanocentury, KAIST
Daejeon 305-701 (Republic of Korea)
E-mail: sangouk.kim@kaist.ac.kr

J.-H. Lee, Prof. J.-B. Yoon
Department of Electrical Engineering
KAIST, Daejeon 305-701 (Republic of Korea)

S.-W. Son, Prof. H. Jeong
Department of Physics
KAIST, Daejeon 305-701 (Republic of Korea)

Dr. S. Lee
LCD R & D Center
Samsung Electronics
San#24 Nongseo-dong
Giheung-gu, Yongin-city
Gyeonggi-do 446-711 (Republic of Korea)

D. I. Lee, S. U. Kwak
AP System Inc.
605 Jung-Ri, Dongtan-Myun
Hwasung, Kyungki-do 445-813 (Republic of Korea)

Prof. H. Shin
School of Advanced Materials Engineering
Kookmin University
Jeongneung-dong, Seongbuk-gu
Seoul 136-702 (Republic of Korea)

Prof. O. D. Lavrentovich
Liquid Crystal Institute
and Chemical Physics Interdisciplinary Program
Kent State University
Kent, Ohio 44242 (USA)

DOI: 10.1002/adfm.200900121

© 2009 WILEY-VCH Verlag GmbH & Co. KGaA, Weinheim

ordering of the soft nanodomains of block copolymers is frequently associated with a high density of defects. To date, enormous research efforts have been devoted to promote the lateral ordering of nanodomains. Typical methods include the application of an external electric, magnetic or shear field,[17–19] directional solidification under a temperature/concentration gradient,[20,21] and directed assembly onto chemically/topographically patterned substrates.[22–26] Most of these approaches, however, require a multi-step process and complicated facilities.

Here, we present spontaneous lamellar alignment in thickness-modulated block copolymer films as a simple and scalable principle to prepare a well-aligned lamellar morphology. Although the aligning effect of the thickness gradient has been previously noticed,[27] the mechanisms of this interesting phenomenon remain unclear. In order to establish this mechanism, we explore the relevant experimental conditions under which alignment takes place, by preparing thickness-modulated block copolymer films via various methods such as solution dropping, dewetting-induced micropatterning and thermal imprinting. After sufficient thermal annealing at high temperature, a well-ordered lamellar morphology aligned along the thickness gradient was observed in the thickness-modulated films, regardless of the film preparation method. The spontaneous lamellar alignment behavior has been carefully examined by real-time atomic force microscopy (AFM) measurements. Based on the experimental data, we propose that the spontaneous alignment in a lamellar block copolymer film with thickness gradient is caused by the so-called ''geometrical anchoring'' phenomenon, originally considered for liquid crystal alignment under a non-flat geometry of confinement. The geometrical anchoring selects the state with the lamellae oriented parallel to the thickness gradient as the sole ground state of the system. The alignment is assisted by motion of linear defects from thicker to thinner parts of the film.

2. Results and Discussion

The spontaneous lamellar alignment behavior is schematically described in Figure 1a. A thickness-modulated film of symmetric polystyrene-*block*-poly(methyl methacrylate) (PS-*b*-PMMA, molecular weight: 104 kg mol^{-1}, lamellar period: 48 nm) was prepared on a neutrally modified substrate. The neutral substrate surface has the same interfacial tension to PS and PMMA components, such that, without any preferential segregation of a particular component (PS or PMMA) at the film-substrate interface, the thin film confinement develops a surface perpendicular oriented lamellar morphology in an equilibrium morphology.[28] The thickness-modulated block copolymer film was prepared upon a neutral substrate via either dewetting-induced self-organized micropatterning or thermal imprinting using a hard mold or, alternatively, by solution dropping upon a tilted neutral substrate (see the Experimental section and the Supporting Information, Fig. S1). Regardless of the preparation method, spontaneous lamellar alignment occurred if the thickness gradient of the prepared film was higher than a critical value, typically in a range of 3–5°. Upon thermal annealing at 220 °C, the lamellae became vertically oriented throughout the film thickness on the neutral substrate surface. However, the lateral ordering of lamellar nanodomains consisted of randomly oriented lamellae with a high density of defects in the early stage of annealing. This morphology is typical of a lamellar block copolymer film self-assembled upon a homogeneous neutral substrate. Annealing proceeds through three processes: i) motion of linear defects, dislocations and disclinations, from the thicker to thinner parts of the film; ii) annihilation of linear defects of opposite ''topological charge''; and iii) reorientation of the lamellae along the thickness gradient. This directional growth of the well-aligned lamellar domain is a unique feature exclusively observed in the thickness-modulated part of the film. Prolonged thermal annealing did not yield any preferential alignment of nanodomains in the uniform thickness region of the film.

Figure 1b–e shows sequential AFM images of nanoscale lamellar morphology taken at a thickness-modulated part of the film (marked by the square in Fig. 1a) during the thermal

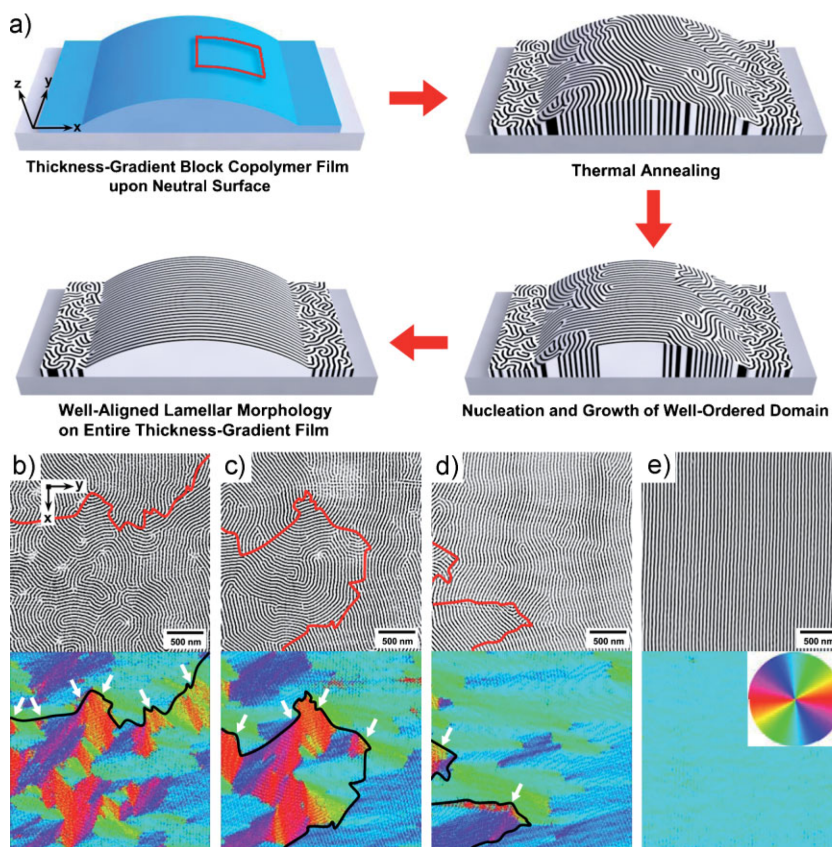

Figure 1. a) Schematic illustration of spontaneous lamellar alignment in a thickness-modulated block copolymer film. Consecutive real-time AFM images (top) and false-color lamellar orientation maps (bottom) of PS-*b*-PMMA films annealed at 220 °C in a vacuum for b) 120, c) 150, d) 180, and, e) 210 min. The degree of lamellar alignment is visualized by the false-color orientation maps.

© 2009 WILEY-VCH Verlag GmbH & Co. KGaA, Weinheim

WILEY InterScience DISCOVER SOMETHING GREAT

annealing process. To observe the real-time morphology evolution, nondestructive AFM imaging was used. The false-color map located below each AFM image presents the distribution of lamellar orientation according to color variation, as indicated in the inset of Figure 1e. This orientation map provides a straightforward visualization of lamellar grains. Owing to the clear contrast in the defect density between the well-aligned lamellar region and randomly oriented lamellar region, the directional growth of the well-aligned domain could be easily recognized. The white arrows indicate the boundary between the well-aligned region and randomly oriented region propagating along the *x*-direction. This boundary separates the regions with low (top) and high (bottom) defect densities. In the well-aligned lamellar region, the dominant defects were dislocations, which did not disturb the alignment of neighboring lamellae significantly. By contrast, the randomly oriented lamellar regions also feature, in addition to dislocations, linear defects in the field of normals to the lamellae, the so-called disclinations. In addition to motion and annihilation of defects, annealing is accompanied by gradual reorientation of the lamellae along the thickness gradient. Such a reorientation is clearly visible in the top left corner of Figure 1b–e, as the lamellae are realigned along the *x*-axis. After sufficient annealing, the well-aligned lamellar domain dominated the entire film, yielding a highly aligned lamellar morphology over a broad area (Figure 1d and e).

Figure 2b and c display tiled scanning electron microscopy (SEM) images of the cryo-fractured cross-section of the thickness-modulated block copolymer films (marked by the square in Fig. 2a) in the early stage (at 220 °C for 60 min) and in the middle of thermal annealing (at 220 °C for 150 min), respectively. The false-color map below each image shows the distribution of lamellar orientation in the film plane. As shown in Figure 2b, the in-plane morphology consisted of randomly oriented lamellae in the early stage of annealing. The density of topological defects was extremely high over the entire area of the film. After thermal annealing (Fig. 2c), the number of defects decreased remarkably over the entire film. In particular, the thicker part of the film (left side of the image) exhibits a well-ordered lamellar morphology highly aligned along the thickness gradient. The red line denotes the front boundary of the self-aligned lamellar domain propagating along the thickness gradient. Figure 2d presents the thickness profiles of a thickness-modulated film before and after thermal annealing. A thickness-modulated film was cryo-fractured into two pieces in liquid nitrogen. One piece of the film was sufficiently annealed at 220 °C for 7 days, while another piece was not annealed. The thickness profiles of the annealed and un-annealed films were measured at the fractured part of the films by cross-sectional SEM observations. A comparison of the profiles revealed that, despite the remarkable alteration of the nanoscale morphology, no significant variation of the height profile occurred during the prolonged annealing process. This confirmed that the spontaneous lamellar alignment cannot be attributed to thermal flow or thermal deformation.

Our experimental observations show that, in the block copolymer film with thickness gradient, the lamellae invariably aligning themselves parallel to the direction of the thickness gradient. Although it is clear that this spontaneous alignment occurs through the directional growth of well-ordered domains, it is not clear why the lamellae end up being parallel to the thickness gradient in the equilibrium state. We propose that the mechanism is related to the balance of the elastic and surface anisotropic

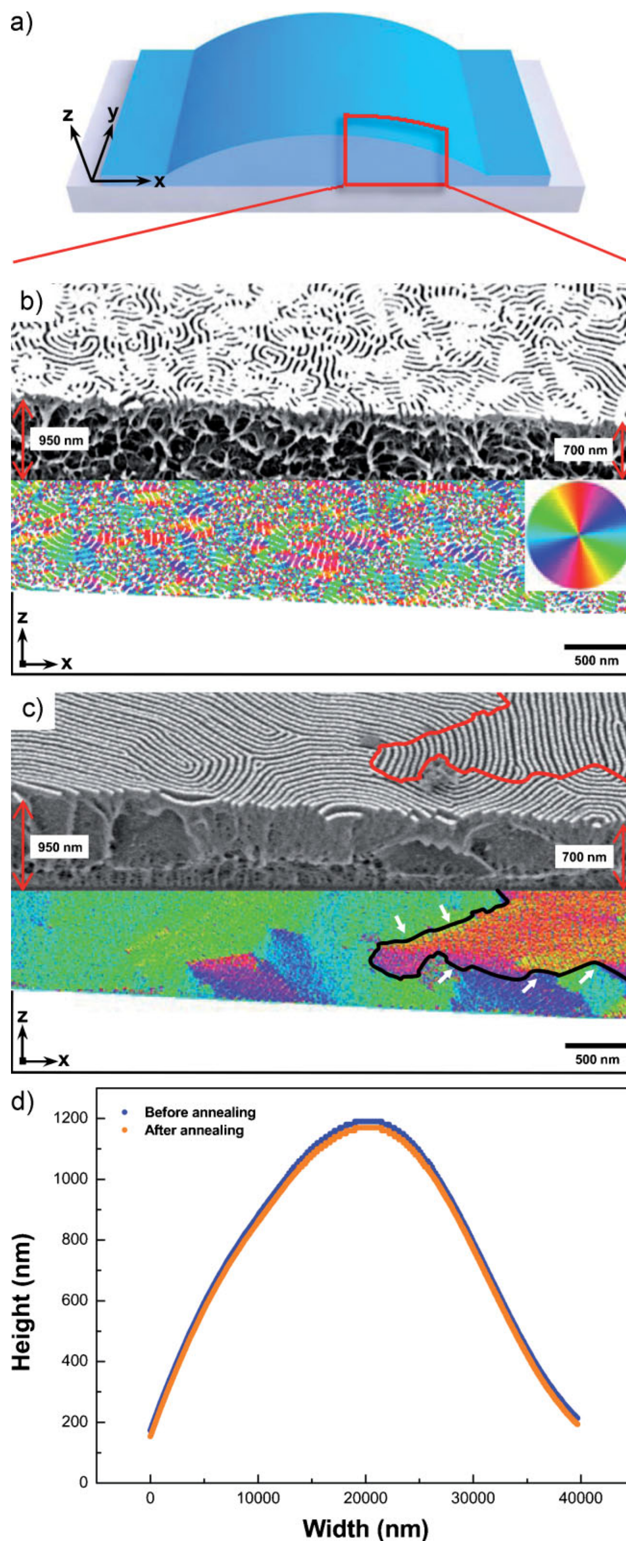

Figure 2. Tilted cross-sectional SEM images (top) and false-color lamellar orientation maps (bottom) of a) thickness-modulated BCP film, b) in the early stage (220 °C for 60 min), and c) in the middle of thermal annealing (220 °C for 150 min). d) The thickness profiles of a thickness-modulated film before and after thermal annealing (220 °C for 7 days). Despite prolonged thermal annealing, the height profile did not show significant variation.

WILEY InterScience DISCOVER SOMETHING GREAT

© 2009 WILEY-VCH Verlag GmbH & Co. KGaA, Weinheim

properties of the block copolymer system, similar to the phenomenon of "geometrical anchoring" introduced some time ago for the somewhat different system of a nematic liquid crystal.[29]

The surface anisotropy of molecular forces is responsible for the phenomenon of surface anchoring, that is, preferential orientation of the lamellas with respect to the free surface. In our case, as clearly seen in the experiments, surface anchoring maintains the normal $\mathbf{n}$ ($\mathbf{n} = -\mathbf{n}$, $\mathbf{n}^2 = 1$) to the block copolymer lamellae in the plane of the bottom neutral substrate and the top free surface, an air-polymer interface.[28] During the thermal annealing performed at 220 °C under vacuum, the free vacuum surface is known to have an identical interfacial tension to the PS and PMMA components.[30] Thus, the lamellae became oriented perpendicular to the top vacuum-polymer interface as well as the bottom polymer-neutral substrate interface during the thermal annealing process.

When the two bounding surfaces are flat and parallel to each other (and to the coordinate plane xy in Fig. 3a), the system is in a degenerate state, as any uniform in-plane orientation $\mathbf{n} = (n_x, n_y, 0)$ would correspond to the energy minimum of the system. Imagine now that the top (free) bounding surface is tilted by an angle γ with respect to the bottom plate, around the y-axis (Fig. 3b and c). It is easy to see that the tilt lifts the degeneracy of the states with arbitrary in-plane orientation of $\mathbf{n}$; it is only the state $\mathbf{n} = (0, 1, 0)$ that corresponds to the elastically undistorted state and, thus, to the energy minimum of the system; in all other states, the lamellae are bent, and $\mathbf{n}$ varies in space.

To consider the mechanism in a more quantitative manner, we present the lamellar block copolymer free energy of distortions in the phenomenological form used in the theory of a one-dimensionally periodic smectic A liquid crystal,

$$f = \tfrac{1}{2}K_1(div\mathbf{n})^2 + \tfrac{1}{2}B\varepsilon^2, \tag{1}$$

where K_1 is the splay elastic constant of the director $\mathbf{n}$ and B is the Young's modulus of relative layers dilations ε. This form has been used in the past by a number of research groups to describe systems such as PS-*b*-PMMA.[31,32] The typical values of the two elastic constants in PS/PMMA system with a period $d_0 = 50$ nm is $K_1 \approx 100$ pN and $B \approx 10^5$ J m^{-3}.[32] The ratio of the two elastic constant introduces an intrinsic material parameter having length $\lambda = \sqrt{K_1/B}$ on the order of a lamellar period d_0. When the system is distorted over distances much larger that λ (for example, for distortion regions far away from the disclination cores), the lamellae tend to preserve their equidistance;[33] the dilation term can then be disregarded and only the splay curvature term is retained for consideration. The last regime is appropriate to discuss the effects of the thickness gradient on the lamellar orientation when the thickness of the film h is much larger than λ.

Let θ be the polar angle between the director $\mathbf{n}$ and the coordinate z-axis normal to the bottom substrate. For a flat sample, the boundary conditions read $\theta(z=0) = \theta_b = \pi/2$ at the bottom and $\theta(z=h) = \theta_t = \pi/2$ at the top (Fig. 3a). Let us now assume that the top surface is tilted with respect to the bottom one by an angle γ around the y-axis (Fig. 3). If the director is kept parallel to the tilted surface because of the tangential surface anchoring, then the value of the angle $\theta(z=h)$ depends on the tilt angle γ and the azimuthal parameter φ_0, that is, the angle between $\mathbf{n}$ and the x'-axis in the tilted upper plane (Fig. 3b). The angle $\theta(z=h)$ in the tilted geometry can be found by writing the z-component of the director in terms of the angles γ and the azimuthal parameter φ_0, i.e., $\cos\theta|_{z=h} = \sin\gamma\cos\varphi_0$. Therefore, the boundary condition for the polar angle at the tilted surface reads $\theta(z=h) = \arccos(\sin\gamma\cos\varphi_0)$. To find the free energy F per unit area of the film, we assume that the polar angle does not depend on the two in-plane coordinates x and y, i.e., $\theta = \theta(z)$. Minimization of the splay term in the free energy density, Equation (1), yields the bulk equilibrium equation $\partial^2\theta/\partial z^2 = 0$ and a solution that satisfies the two boundary conditions, $\theta(z) = \alpha z + \pi/2$, where $\alpha = \arcsin(\sin\gamma\cos\varphi_0)/h$. Integrating the splay energy density over the local thickness of the film, one finds the elastic energy per unit area of the film,

$$F = \frac{K_1}{2h}\arcsin^2(\sin\gamma\cos\varphi_0) \tag{2}$$

The energy reaches its absolute minimum when $\varphi_0 = \pm\pi/2$, which corresponds to uniform lamellar orientation with $\mathbf{n}$ perpendicular to the thickness gradient and parallel to the y-axis (Fig. 4). For small tilts, the energy can be rewritten as

$$F = \frac{K_1\gamma^2}{2h}\cos^2\varphi_0 \tag{3}$$

where the quantity $K_1\gamma^2/h$ plays the role of effective surface anchoring, which keeps the lamellae parallel to the direction of the thickness gradient. As can be readily observed, the steeper the film profile (larger γ), the stronger is the force turning $\mathbf{n}$ towards the y-axis (Fig. 4). Of course, the model above produces only an approximate picture of the alignment effect, as it neglects any non-local effects, the fact that γ in a real system is coordinate-dependent, the actual kinetics through defect annihilation, etc.

The above mechanism can be called "geometrical anchoring"[29] as it stems from the tendency of the system to minimize its overall

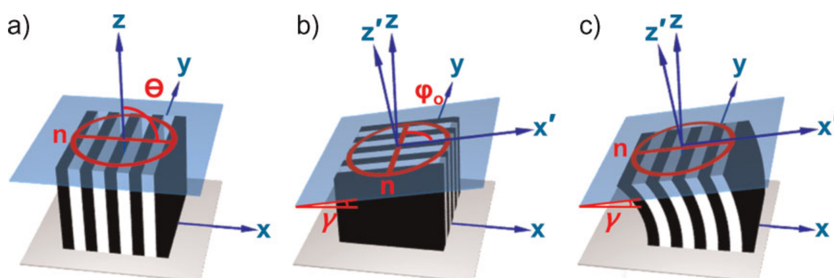

Figure 3. Schematic illustration of lamellar morphology according to the boundary tilting of block copolymer films. Normal $\mathbf{n}$ to the lamellae is tangentially anchored to the top and bottom boundaries of the block copolymer film of a uniform thickness (a) and of varying thickness (b). In the uniform film, the orientation of n is degenerate in the xy-plane; in the film with the top plate tilted about the y-axis, $\mathbf{n}$ tends to be parallel to y to prevent splay deformation of the lamellae; whenever $\mathbf{n}$ deviates from the direction of the y-axis, the layers are bent (c).

© 2009 WILEY-VCH Verlag GmbH & Co. KGaA, Weinheim

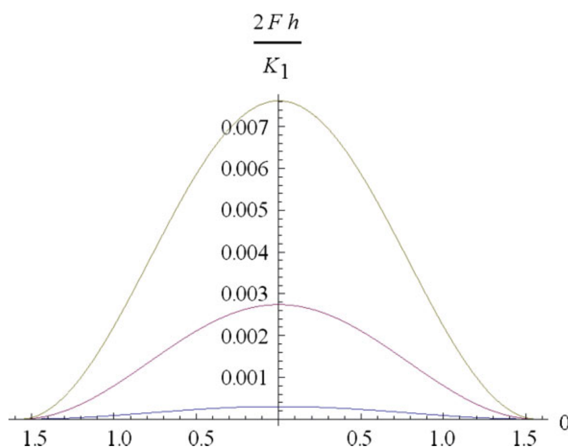

Figure 4. Plot of the surface anchoring function $2Fh/K_1 = \arcsin^2(\sin\gamma\cos\varphi_0)$ *vs.* φ_0 (in radians) for three different values of the tilting angle γ: 1° (bottom), 3° (middle) and 5° (top).

elastic energy under non-flat geometry of confinement. The effect of geometrical anchoring is not related to physical treatment of the substrate, such as rubbing or creation of a special corrugated profile, discussed by Tsori and Andelman.[32] The bounding surfaces might be smooth and uniform with no in-plane anisotropy in their properties; all that is needed for the geometrical anchoring mechanism to align the lamellae is a thickness gradient of the film. A similar effect has been considered for nematic liquid crystals between two isotropic media[29] and for the droplets of liquid crystalline solutions of DNA with free surface.[34]

In the theoretical analysis, the tilting angle γ turned out to be a significant parameter for the spontaneous alignment behavior. We experimentally investigated the spontaneous lamellar alignment, varying the tilting angle of the thickness gradient. Figure 5 compares two SEM images of thickness-modulated films having different tilting angles γ in their microscale morphology. In the film shown in Figure 5a, in which the γ value was approximately 1°, although the defect density shows a remarkable contrast between thick and thin parts of the film, no preferential lamellar alignment was observed. In contrast, in the film having a higher γ value of approximately 3°, spontaneous lamellar alignment occurred (Fig. 5b). We note that the effective surface anchoring parameter, $K_1\gamma^2/h$, for 3° is nine times as large as that for 1°. Our investigation of dozens of samples revealed that the critical γ value for spontaneous alignment was approximately 3–5°. Note that since the nanoscale alignment is determined mostly by γ rather than by the width of the film, the morphology of micropatterned films can be controlled over large areas provided that the value of γ is kept above the critical value at the stage of film preparation (Supporting Information, Table S1). This lends scalability to our approach, enabling control over the alignment of nanoscale morphology by adjusting the much larger microscale structure. Furthermore, a well-aligned, surface perpendicular lamellar morphology having an extremely high aspect ratio in the film thickness direction as well as the film plane direction could be created.[27]

With the experimental values of the tilt angle at which the alignment through the thickness gradients become efficient, $\gamma = 3–5°$ and $h = 500$ nm, and with the typical $K_1 = 100$ pN, one finds that the corresponding geometrical anchoring coefficient is $K_1\gamma^2/h \sim 10^{-6}\ J/m^2$, close to the typical values of surface anchoring coefficients in systems with orientational order such as liquid crystals.[33] Note that the mechanism of geometrical anchoring considered above implies that the normal **n** to the lamellae is tangential to the block copolymer-air and block copolymer-substrates interfaces. If the energy cost to deviate **n** away from these surfaces (i.e., to make a tilted or planar alignment of lamellae at the interfaces) is much smaller than $K_1\gamma^2/h \sim 10^{-6}\ J/m^2$, then the geometrical anchoring mechanism would not cause an aligning effect as described above. A simple consideration below shows that, typically, the surface anchoring of a lamellar block copolymer system that is responsible for the tangential anchoring of **n** at the interfaces is much stronger than $K_1\gamma^2/h$. First, note that the tilted orientation of **n** with respect to the surface implies some reorganization of the molecular structure near the interface. If the surface tension σ_0 is much larger than the energy Bd_0 of layers breaking, then this restructuring might involve melting of layers to preserve the smoothness and minimal area of the interface. The corresponding energy cost is on the order of $Bd_0 \sim 5 \cdot 10^{-3}\ J/m^2$, much higher than the typical value of the "geometrical" anchoring coefficient $K_1\gamma^2/h \sim 10^{-6}\ J/m^2$. If, on the other hand, $\sigma_0 \ll Bd_0$ (this condition might be fulfilled at the free surface), then the surface adopts a rippled profile with surface anchoring potential $\sigma(\theta) = \sigma_{||}|\sin\theta| + \sigma_\perp|\cos\theta|$, where $\sigma_{||}$ and $\sigma_\perp$ are two surface tension coefficients. Although we do not know the exact values of $\sigma_{||}$ and $\sigma_\perp$, it is expected that their typical values are on the order of $10^{-3}\ J/m^2$ and are, thus, larger than the typical values of $K_1\gamma^2/h$. These considerations demonstrate that the assumption of **n** being in the plane of the bounding surfaces is justified. Of course, the most cogent argument is that the experimental data on the studied system in flat and gradient geometries clearly demonstrate that the lamellae are perpendicular to the bounding surfaces, i.e., that **n** is tangential to these surfaces.

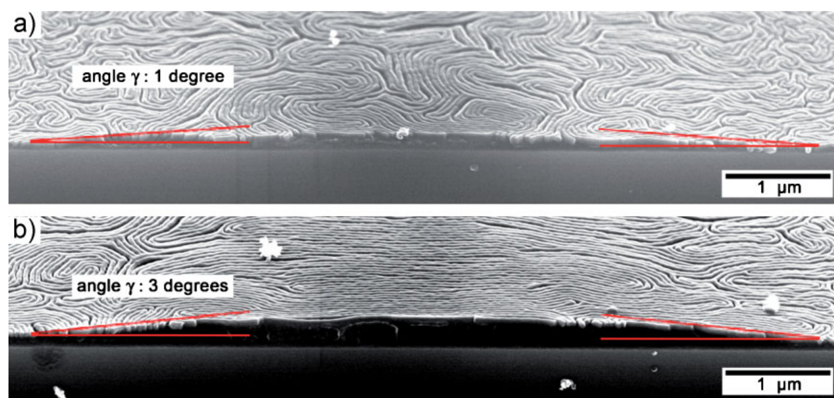

Figure 5. Tilted side-view SEM images of fractured thickness-modulated block copolymer films annealed at 220 °C for 10 days. Self-alignment of the lamellae did not occur (a) for a film with a mild thickness gradient (tilting angle γ: 1°) but occurred (b) for a film with a steeper thickness gradient (tilting angle γ: 3°).

© 2009 WILEY-VCH Verlag GmbH & Co. KGaA, Weinheim

As described above, spontaneous lamellar alignment is assisted by motion of the defects such as dislocations and disclinations from the thickest part of the film towards the thinnest part, along the thickness gradient. This signifies that the thicker part of the block copolymer film evolves toward its equilibrium morphology more rapidly. There are two mechanisms contributing to this effect. One is associated with the experimentally observed tendency of thicker films to exhibit faster coarsening dynamics as compared to the thinner films, an effect that might be associated with the role of surfaces and pinning of the defects at the surface irregularities, which will be discussed in the next paragraph. The second effect is in the obvious tendency of a vertical defect line to move from a thicker part of the film to the thinner part, as such a motion decreases the length of the defect and, thus, the associated elastic energy. Since lamellae were oriented perpendicular to the neutral substrate surface, the linear defect penetrates the entire film thickness, and its elastic energy is, thus, proportional to the film thickness, $E(x) \sim Kh(x)$. Since the local thickness depends on the horizontal coordinate, in linear approximation $h(x) \sim const - \gamma x$, the dislocations and disclinations are subject to a lateral force $|-\partial E(x)/\partial x| \sim K\gamma$ that drives them towards the thinner part of the film. Note that this mechanism is also helping in aligning the lamellae along the thickness gradient: since climb of dislocations is easier than their glide, domains with lamellae oriented along the thickness gradients would anneal faster than the domains with lamellae perpendicular to the thickness gradient.

In order to obtain insight into the behavior associated with the thickness of the film of zero tilt, uniform block copolymer films with various thicknesses were prepared and their defect annihilation behavior was investigated. From domain coarsening dynamics, it is generally known that the defect density $d(t)$ decreases with time t following the power law $d(t) \sim t^{-\nu}$ (ν kinetic exponent).[35] In mean-field arguments for nematic liquid crystals, the defect annihilation rate is considered to be proportional to the probability of binary collisions between oppositely charged defects, $d(d(t))/dt \sim d(t)^2$; in this case, $\nu = 1$.[36] A smectic liquid crystalline system has more restrictions in defect motions due to its layered structure. Thus, the kinetic exponent ν is usually less than 1. The kinetic exponent value of ν for block copolymer thin films may have a broad range of values. This depends on various parameters, such as the nature of nanoscale morphology (surface parallel cylinders or surface perpendicular lamellae), molecular weight of block copolymers, and film thickness.[37] Harrison reported a ν value of 0.5 for a two-dimensional stripe pattern of single layered cylindrical block copolymers.[38] Ruiz reported a ν value of 0.22 for block copolymer thin films having surface perpendicular oriented lamellar morphology.[39]

In our experiments, uniform lamellar block copolymer films with various film thicknesses ranging from 100 to 400 nm were prepared upon neutrally treated substrates via spin-coating. After a predetermined period of thermal annealing at 220 °C, the nanoscale morphology at the film surface was examined by plane-view SEM measurements. As shown in Figure 6a–c, as the film thickness increased, the defect density became lower after the same annealing time. The density of disclinations $d(t)$ was measured as a function of time (t). Figure 6d shows the average distance between the neighboring disclinations $d(t)^{-1/2}$ plotted against annealing time on a logarithmic scale. The linear regression in the logarithmic scale plot provided kinetic exponent values of $\nu_{100} = 0.04$, $\nu_{200} = 0.06$, $\nu_{300} = 0.08$, and $\nu_{400} = 0.12$ for film thicknesses of 100, 200, 300 and 400 nm, respectively. The obtained kinetic exponent values were roughly proportional to the thicknesses of the block copolymer films. This revealed that, as the block copolymer film became thicker, the defect annihilation became more rapid. This interesting behavior may be understood as the result of pinning of the defects at the block copolymer film-substrate interface. The interfacial area-to-volume ratio of block copolymer film is inversely proportional to the film thickness. As a consequence, in thick films, pinning of defects at surface irregularities might be a less significant obstacle for defect annihilation as compared to thin films. This variation of the defect annihilation rate with

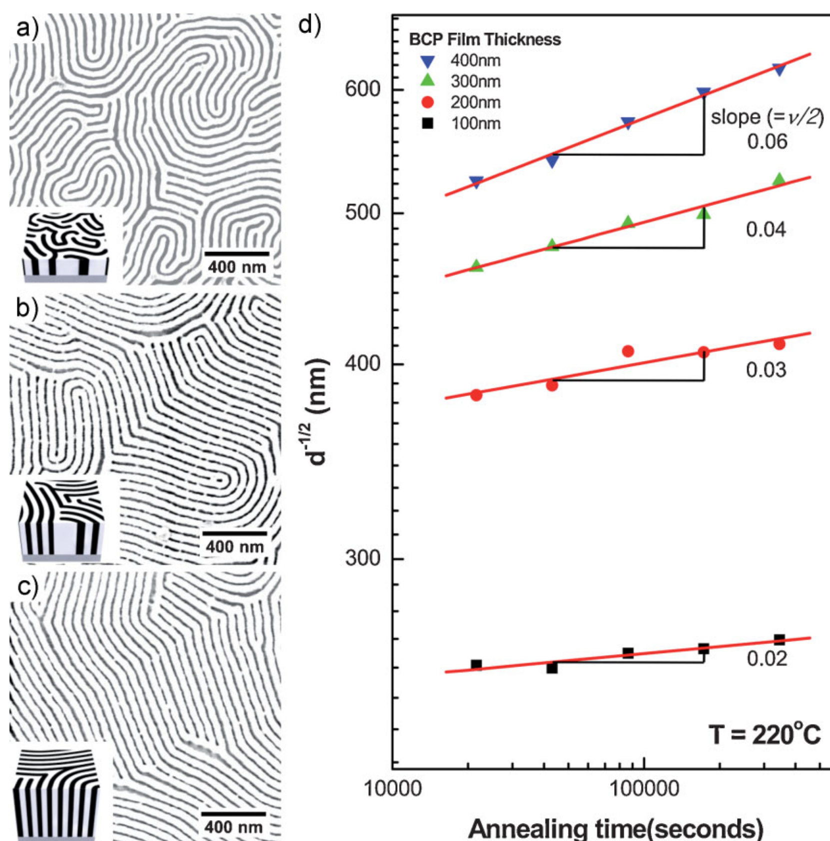

Figure 6. Plane-view SEM images of block copolymer thin films with uniform thicknesses of a) 100, b) 300, and, c) 400 nm after annealing at 220 °C for 96 h. d) Average spacing between neighboring disclinations ($d^{-1/2}$, d: disclination density) plotted against annealing time in logarithmic scales. The kinetic exponent of the defect annihilation obtained by linear regression was roughly proportional to the block copolymer film thickness.

© 2009 WILEY-VCH Verlag GmbH & Co. KGaA, Weinheim

WILEY InterScience DISCOVER SOMETHING GREAT

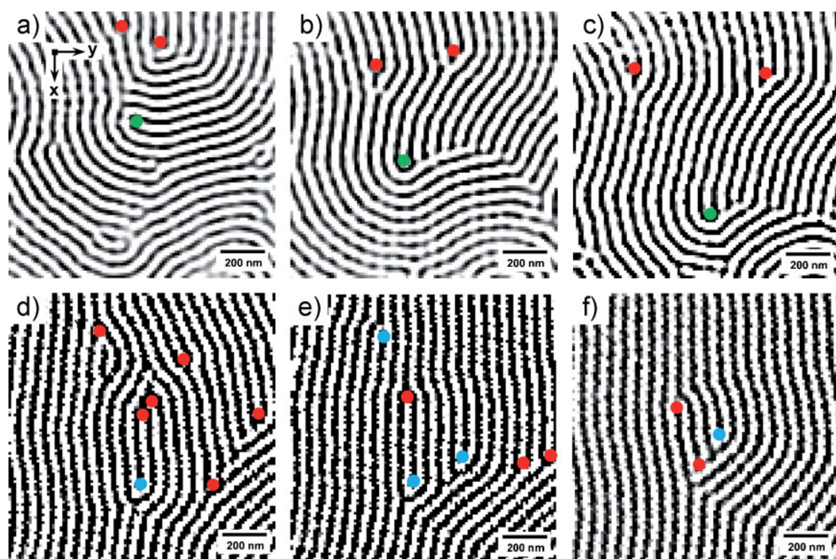

Figure 7. Consecutive time-lapse AFM images capturing the preferential movement of disclinations (a–c and dislocations d–e) along the thickness gradient. The thermal annealing was performed at 220 °C in a vacuum for 120 min (a and d), for 125 min (b and e), and for 130 min (c and f) (red dots: PMMA core dislocations, blue dots: PS core dislocations, green dots: $+1/2$ disclination).

film thickness gives rise to the growth of well-aligned domain from the thickest part of the film and propagation along the thickness gradient. We note that when the tilting angle γ was less than the critical value for spontanous alignment, the variation of defet annihilation rate simply resulted in the variation of defect density along thickness gradient without any preferential lamellar alignment (Figure 5a).

The directional growth of well-ordered lamellar domain along the thickness gradient accommodates the preferential movement of topological defects in the same direction. Figure 7a–f shows a series of AFM images taken at the edge of a well-aligned domain propagating along the thickness gradient (x-direction). In Figure 7a, the lamellae associated with a $+1/2$ disclination, whose core is marked by a green dot, were oriented along the y-direction. Upon further annealing, the disclination moved toward the x-direction along with the domain propagation and, at the same time, the associated lamellae were redirected along the x-direction (Figs. 7b and c). Figure 7d–f presents sequential AFM images showing the preferential movement of dislocations along the domain propagating direction. Since defects are annihilated via coupling with oppositely signed defects, the defects propagating along with the front boundary of the growing domain may eventually merge with a counter defect located outside of the growing domain.

3. Conclusions

We have demonstrated spontaneous lamellar alignment as a generalized behavior of thickness-modulated block copolymer films. Thickness-modulated block copolymer films were prepared by various methods, such as dewetting-induced patterning, thermal imprinting, and solution dropping. Geometrical anchoring, which is caused by the tendency to minimize the overall elastic energy under a non-flat geometry of confinement, induced spontaneous alignment of block copolymer lamellae along the thickness gradient. Real-time AFM measurement during isothermal annealing visualized textural reorganization through i) preferential movement of defects along the thickness gradient from the thick to the thin parts of the film; ii) defects annihilation (with a rate that is higher in thick films, as compared to thin films); and iii) realignment of the lamellae along the thickness gradient. The thickness gradient imposes unique orientation of the lamellae (parallel to the gradient) through the geometrical anchoring mechanism. Exploiting this interesting self-aligning principle, a highly aligned nanoscale lamellar pattern could be prepared without any prepatterning process or external field. The simple process of micropatterning a block copolymer film and subsequent isothermal annealing produced a well-aligned lamellar morphology over a large area. The ability to control the morphology at a nanoscale level by manipulating much larger microscale morphology may provide a useful platform for large-scale nanopatterning processes.

4. Experimental

Neutral Modification of Substrate Surface: The surface of the silicon substrate was neutrally modified by a polystyrene-*ran*-poly(methyl methacylate) (PS-*r*-PMMA, number-average molecular weight, $\overline{M}_n$: 95 kg mol^{-1}) random copolymer brush so as to provide identical interfacial tensions for the PS and PMMA blocks [6,28]. First, the silicon wafer was immersed in a piranha solution (7:3 mixture of H_2SO_4 and H_2O_2) for 1 h at 110 °C. The acid-treated silicon wafer was subsequently washed with deionized water. The PS-*r*-PMMA brush layer was deposited by spin-coating a thin film of the random brush and subsequent thermal annealing at 160 °C for 48 h in a vacuum. After surface modification, thickness-gradient films of a symmetric diblock copolymer, polystyrene-*block*-poly(methyl methacrylate) (PS-*b*-PMMA, number-average molecular weight, $\overline{M}_n$, of PS block: 52 kg mol^{-1}, $\overline{M}_n$ of PMMA block: 52 kg mol^{-1}, Polymer Source, Inc.) were prepared by three methods, as described below (Supporting Information, Fig. S1). After film preparation, thermal annealing was conducted at 220 °C to produce a well-aligned lamellar morphology in the thickness-modulated region.

Solution Dropping upon Tilted Neutral Substrate: Solution dropping is a very simple and useful method to prepare a thickness-modulated block copolymer film. A droplet of block copolymer solution (2 wt.%, dissolved in toluene) was dropped over a 45° tilted, neutrally treated silicon wafer. One bump, having a straight-line shape, was prepared after drying. (Supporting Information, Fig. S1a).

Dewetting-Induced Self-Organized Patterning: Periodic thickness modulation can be achieved by deweting induced self-organized patterning [27,40]. A 0.5–4 wt.% block copolymer solution in toluene was confined in the gap (5–80 μm) between a slide glass (top-side) and a neutrally treated silicon substrate (bottom-side). The step motor was employed to draw the glass plate located on the top side with a constant velocity (2–40 μm s^{-1}). The polymer residue deposited at the evaporating front of the polymer solution temporarily pinned the receding contact line such that the solution edge underwent successive cycles of pinning and depinning. A block

WILEY InterScience DISCOVER SOMETHING GREAT
© 2009 WILEY-VCH Verlag GmbH & Co. KGaA, Weinheim

copolymer film, having a periodic thickness modulation, was generated from the receding edge of the polymer solution (Supporting Information, Fig. S1b).

Thermal Imprinting: A photoresist pattern consisting of a periodic bump structure was prepared by conventional photolithography and a photoresist thermal flow process. A copper seed layer (10 nm) was thermally evaporated upon the photoresist pattern. A nickel stamp having an inverse-morphology of the photoresist pattern was replicated by an electroplating method. After electroplating, the silicon wafer and photoresist pattern were completely removed. Silicon oxide film (10 nm) was deposited upon the nickel stamp surface by plasma enhanced chemical vapor deposition (PECVD) and the silica treated surface was modified with an octadecyltrichlorosilane (OTS) self-assembled monolayer (SAM) for anti-adhesion. A thermal imprint process was performed upon the uniform block copolymer film spin-coated on the neutrally treated silicon wafer. (50 bar, 120 °C, 10 min) (Supporting Information, Fig. S1c).

Real-Time Atomic Force Microscopy (AFM) and Scanning Electron Microscopy (SEM): The plane-view of the thickness-modulated block copolymer thin film was scanned by AFM (Seiko Instruments) in the dynamic force microscopy (DFM) mode using an SI-DF3 cantilever (spring constant: 1.6 N m^{-1}, resonance frequency: 26 kHz). The AFM images were obtained in a vacuum (10^{-6}–10^{-7} torr) at room temperature. The morphology of the block copolymer nanostructure was imaged using a Hitachi S-4800 SEM with a field emission source at 1 kV.

Acknowledgements

We would like to thank Dr. Meesoon Ha for useful discussions. This work was supported by the second stage of the Brain Korea 21 Project, the National Research Laboratory Program (R0A-2008-000-20057-0, R0A-2007-000-20105-0), the 21st Century Frontier Research Program (Center for Nanoscale Mechatronics and Manufacturing, 08K1401-01010), and KAIST EEWS (Energy, Environment, Water, and Sustainability) Initiative (EEWS0903), funded by the Korean government. ODL acknowledges the support of grants from the US NSF (DMR0504516) and the State of Ohio (CMPND and RC-SAM). Supporting Information is available online from Wiley InterScience or from the author.

Received: January 22, 2009
Revised: March 16, 2009
Published online: June 22, 2009

[1] G. M. Whitesides, B. Grzybowski, *Science* **2002**, *295*, 2418.
[2] C. Tang, E. M. Lennon, G. H. Fredrickson, E. J. Kramer, C. J. Hawker, *Science* **2008**, *322*, 429.
[3] Y. Lin, A. Böker, J. He, K. Sill, H. Xiang, C. Abetz, X. Li, J. Wang, T. Emrick, S. Long, Q. Wang, A. Balazs, T. P. Russell, *Nature* **2005**, *434*, 55.
[4] D. K. Yoon, M. C. Choi, Y. H. Kim, M. W. Kim, O. D. Lavrentovich, H. T. Jung, *Nat. Mater.* **2007**, *6*, 866.
[5] T. H. Han, J. Kim, J. S. Park, H. Ihee, S. O. Kim, *Adv. Mater.* **2007**, *19*, 3924.
[6] S.-J. Jeong, G. Xia, B. H. Kim, D. O. Shin, S.-H. Kwon, S.-W. Kang, S. O. Kim, *Adv. Mater.* **2008**, *20*, 1898.
[7] D. H. Lee, D. O. Shin, W. J. Lee, S. O. Kim, *Adv. Mater.* **2008**, *20*, 2480.
[8] M. Park, C. Harrison, P. M. Chaikin, R. A. Register, D. H. Adamson, *Science* **1997**, *276*, 1401.
[9] H. C. Kim, X. Q. Jia, C. M. Stafford, D. H. Kim, T. J. McCarthy, M. Tuominen, C. J. Hawker, T. P. Russell, *Adv. Mater.* **2001**, *13*, 795.
[10] K. W. Guarini, C. T. Black, Y. Zhang, H. Kim, E. M. Sikorski, I. V. Babich, *J. Vac. Sci. Technol. B* **2002**, *20*, 2788.
[11] M. Park, P. M. Chaikin, R. A. Register, D. H. Adamson, *Appl. Phys. Lett.* **2001**, *79*, 257.
[12] R. R. Li, P. D. Dapkus, M. E. Thompson, W. G. Jeong, C. Harrison, P. M. Chaikin, R. A. Register, D. H. Adamson, *Appl. Phys. Lett.* **2000**, *76*, 1689.
[13] J. Y. Cheng, C. A. Ross, V. Z. H. Chan, E. L. Thomas, R. G. H. Lammertink, G. J. Vancso, *Adv. Mater.* **2001**, *13*, 1174.
[14] K. Naito, H. Hieda, M. Sakurai, Y. Kamata, K. Asakawa, *IEEE Trans. Magn.* **2002**, *38*, 1949.
[15] W. A. Lopes, H. M. Jaeger, *Nature* **2001**, *414*, 735.
[16] J. K. Li, S. Zou, D. A. Rider, I. Manners, G. C. Walker, *Adv. Mater.* **2008**, *20*, 1989.
[17] T. L. Morkved, M. Lu, A. M. Urbas, E. E. Ehrichs, H. M. Jaeger, P. Mansky, T. P. Russell, *Science* **1996**, *273*, 931.
[18] D. E. Angelescu, J. H. Waller, D. H. Adamson, P. Deshpande, S. Y. Chou, R. A. Register, P. M. Chaikin, *Adv. Mater.* **2004**, *16*, 1736.
[19] Y. Morikawa, S. Nagano, K. Watanabe, K. Kamata, T. Iyoda, T. Seki, *Adv. Mater.* **2006**, *18*, 883.
[20] D. E. Angelescu, J. H. Waller, D. H. Adamson, R. A. Register, P. M. Chaikin, *Adv. Mater.* **2007**, *19*, 2687.
[21] C. De Rosa, C. Park, E. L. Thomas, B. Lotz, *Nature* **2000**, *405*, 433.
[22] S. O. Kim, H. H. Solak, M. P. Stoykovich, N. J. Ferrier, J. J. de Pablo, P. F. Nealey, *Nature* **2003**, *424*, 411.
[23] M. P. Stoykovich, M. Muller, S. O. Kim, H. H. Solak, E. W. Edwards, J. J. de Pablo, P. F. Nealey, *Science* **2005**, *308*, 1442.
[24] S. O. Kim, B. H. Kim, D. Meng, D. O. Shin, C. M. Koo, H. H. Solak, Q. Wang, *Adv. Mater.* **2007**, *19*, 3271.
[25] R. A. Segalman, H. Yokoyama, E. J. Kramer, *Adv. Mater.* **2001**, *13*, 1152.
[26] J. Y. Cheng, A. M. Mayes, C. A. Ross, *Nat. Mater.* **2004**, *3*, 823.
[27] B. H. Kim, D. O. Shin, S.-J. Jeong, C. M. Koo, S. C. Jeon, W. J. Hwang, S. Lee, M. G. Lee, S. O. Kim, *Adv. Mater.* **2008**, *20*, 2303.
[28] P. Mansky, Y. Liu, E. Huang, T. P. Russell, C. Hawker, *Science* **1997**, *275*, 1458.
[29] O. D. Lavrentovich, *Phys. Rev. A* **1992**, *46*, R722.
[30] P. Mansky, T. P. Russell, C. J. Hawker, J. Mays, D. C. Cook, S. K. Satija, *Phys. Rev. Lett.* **1997**, *79*, 237.
[31] K. Amundson, E. Helfand, *Macromolecules* **1993**, *26*, 1324.
[32] Y. Tsori, D. Andelman, *Macromolecules* **2003**, *36*, 8560.
[33] M. Kleman, O. D. Lavrentovich, *Soft Matter Physics: An Introduction*, Springer, NY, USA **2003**.
[34] I. I. Smalyukh, O. V. Zribi, J. C. Butler, O. D. Lavrentovich, G. C. L. Wong, *Phys. Rev. Lett.* **2006**, *96*, 177801.
[35] A. N. Pargellis, P. Finn, J. W. Goodby, B. Yurke, P. E. Cladis, *Phys. Rev. A* **1992**, *46*, 7765.
[36] B. Yurke, A. N. Pargellis, T. Kovacs, D. A. Huse, *Phys. Rev. E* **1993**, *47*, 1525.
[37] R. Ruiz, J. K. Bosworth, C. T. Black, *Phys. Rev. B* **2008**, *77*, 054204.
[38] C. Harrison, D. H. Adamson, Z. Cheng, J. M. Sebastian, S. Sethuraman, D. A. Huse, R. A. Register, P. M. Chaikin, *Science* **2000**, *290*, 1558.
[39] R. Ruiz, R. L. Sandstrom, C. T. Black, *Adv. Mater.* **2007**, *19*, 587.
[40] H. Yabu, M. Shimomura, *Adv. Funct. Mater.* **2005**, *15*, 575.

© 2009 WILEY-VCH Verlag GmbH & Co. KGaA, Weinheim

WILEY InterScience® DISCOVER SOMETHING GREAT